



Excision of Integrated Human Herpesvirus 6A Genomes Using CRISPR/Cas9 Technology

Giulia Aimola,^a Darren J. Wight,^a  Louis Flamand,^{b,c}  Benedikt B. Kaufer^{a,d}

^aInstitut für Virologie, Freie Universität Berlin, Berlin, Germany

^bDivision of Infectious and Immune Diseases, CHU de Quebec Research Center-Laval University, Québec, Canada

^cDepartment of Microbiology, Infectious Disease and Immunology, Faculty of Medicine, Laval University, Québec, Canada

^dVeterinary Centre for Resistance Research (TZR), Freie Universität Berlin, Berlin, Germany

ABSTRACT Human herpesviruses 6A and 6B are betaherpesviruses that can integrate their genomes into the telomeres of latently infected cells. Integration can also occur in germ cells, resulting in individuals who harbor the integrated virus in every cell of their body and can pass it on to their offspring. This condition is termed inherited chromosomally integrated HHV-6 (iciHHV-6) and affects about 1% of the human population. The integrated HHV-6A/B genome can reactivate in iciHHV-6 patients and in rare cases can also cause severe diseases including encephalitis and graft-versus-host disease. Until now, it has remained impossible to prevent virus reactivation or remove the integrated virus genome. Therefore, we developed a system that allows the removal of HHV-6A from the host telomeres using the CRISPR/Cas9 system. We used specific guide RNAs (gRNAs) targeting the direct repeat region at the ends of the viral genome to remove the virus from latently infected cells generated *in vitro* and iciHHV-6A patient cells. Fluorescence-activated cell sorting (FACS), quantitative PCR (qPCR), and fluorescence *in situ* hybridization (FISH) analyses revealed that the virus genome was efficiently excised and lost in most cells. Efficient excision was achieved with both constitutive and transient expression of Cas9. In addition, reverse transcription-qPCR (RT-qPCR) revealed that the virus genome did not reactivate upon excision. Taken together, our data show that our CRISPR/Cas9 approach allows efficient removal of the integrated virus genome from host telomeres.

IMPORTANCE Human herpesvirus 6 (HHV-6) infects almost all humans and integrates into the telomeres of latently infected cells to persist in the host for life. In addition, HHV-6 can also integrate into the telomeres of germ cells, which results in about 80 million individuals worldwide who carry the virus in every cell of their body and can pass it on to their offspring. In this study, we develop the first system that allows excision of the integrated HHV-6 genome from host telomeres using CRISPR/Cas9 technology. Our data revealed that the integrated HHV-6 genome can be efficiently removed from the telomeres of latently infected cells and cells of patients harboring the virus in their germ line. Virus removal could be achieved with both stable and transient Cas9 expression, without inducing viral reactivation.

KEYWORDS HHV-6, iciHHV-6, integration, CRISPR/Cas9, gRNAs, excision

Human herpesvirus 6A and 6B (HHV-6A/B) are closely related betaherpesviruses (1–4). Primary infection with HHV-6B usually occurs within the first 2 years of life. It is the causative agent of the febrile illness roseola infantum (5), which can be accompanied by more severe neurological complications like seizures and encephalitis. HHV-6A infection is believed to occur later in life, but less is known about its epidemiology and clinical manifestations (5–7). Upon primary infection, HHV-6A/B can establish latency, allowing the virus to persist in the host for life (8, 9). While most herpesviruses maintain their genome as a circular episome during latency, HHV-6A/B can integrate into the

Editor Donna M. Neumann, University of Wisconsin-Madison

Copyright © 2023 Aimola et al. This is an open-access article distributed under the terms of the [Creative Commons Attribution 4.0 International license](https://creativecommons.org/licenses/by/4.0/).

Address correspondence to Benedikt B. Kaufer, b.kaufer@fu-berlin.de.

The authors declare no conflict of interest.

Received 22 February 2023

Accepted 23 February 2023

Published 16 March 2023

telomeres to maintain their genome (10–12). Intriguingly, integration can occur not only in somatic cells but also in germ cells. Integration in germ cells can result in individuals carrying the integrated virus in every cell of the body, and they can pass on the integrated virus to their offspring in a Mendelian fashion (10, 13–15). This condition is known as inherited chromosomally integrated HHV-6 (iciHHV-6) and affects about 1% of the world population. HHV-6A/B reactivation in iciHHV-6 individuals and from its latent state has been associated with different clinical manifestations, including heart diseases, encephalitis, and graft-versus-host disease (GvHD) (16–21).

HHV-6A/B have a linear double-stranded DNA genome of approximately 160 kbp. The unique region (U) contains most viral genes and is flanked by two identical direct repeat regions (DRs) of about 8 kbp each (4, 22–24). The DRs also contain telomeric repeat arrays (TMRs) consisting of (TTAGGG)_n repeats identical to the telomeres of humans and all other vertebrates (25–28). These viral TMRs have been previously shown to facilitate the integration of HHV-6A into the host telomeres (29).

Analyses of the integrated virus in iciHHV-6 patients revealed that integration occurs with a specific orientation of the virus genome (30–32). The perfect TMR array (pTMR) on the right DR apparently recombined with the host telomeres. Thereby, longer telomere sequences of several kilobase pairs remain between the virus and the subtelomeres of the host chromosome. At the end of the left DR, long telomeres were observed that correspond to the length of the other telomeres within the host cell (33). Several viral and cellular factors have been investigated (29, 34–39); however, the precise mechanism that facilitates HHV-6 integration remains poorly understood. Until now, it has remained impossible to prevent HHV-6A/B reactivation and/or eliminate the integrated virus from human chromosomes, which we aimed to achieve in this study.

The clustered regularly interspaced short palindromic repeats (CRISPR) and the CRISPR-associated (Cas) protein system are an adaptive immune mechanism in prokaryotes that targets and destroys the nucleic acids of invading viruses (40–43). Among the different CRISPR/Cas classes and groups, the CRISPR type II endonuclease Cas9 of *Streptococcus pyogenes* is one of the best-studied tools (44, 45). This CRISPR/Cas9 system consists of two main components that act together as a complex: the Cas9 endonuclease and a specific guide RNA (gRNA) that drives Cas9 to the desired target sequence (46–49). In the last several years, the CRISPR/Cas9 system has revolutionized the field of genome editing and proved to be a powerful tool for many applications (45–47, 50–53).

In this study, we established a system that allows removal of the integrated HHV-6A genome from the host telomeres using the CRISPR/Cas9 technology. Elimination of the virus genome was achieved in latently infected cells generated *in vitro* and iciHHV-6A patient cells. Both constitutive and transient expression of Cas9 facilitated efficient removal of the virus genome. Successful excision was validated by fluorescence-activated cell sorting (FACS), quantitative PCR (qPCR), and fluorescence *in situ* hybridization (FISH), and the absence of viral reactivation upon excision was assessed by reverse transcription-qPCR (RT-qPCR). Our study provides the first evidence that the HHV-6A genome can be efficiently removed from the host telomeres, an approach that could be used to investigate important features of HHV-6 biology and potential clinical applications in the future.

RESULTS

Generation and characterization of Cas9-expressing cells for the removal of the HHV-6A genome. To establish the removal of the integrated HHV-6A genome with the CRISPR/Cas9 system, we first used a well-characterized 293T cell line harboring the integrated virus genome (293T-6A) (54, 55). These cells were previously infected with HHV-6A expressing green fluorescent protein (GFP) under the control of the major immediate early human cytomegalovirus (HCMV) promoter and harbor two copies of the integrated virus genome. Cas9 was delivered into 293T-6A cells by lentivirus transduction to generate a polyclonal population stably expressing Cas9 upon puromycin selection (293T-6A-Cas9).

Prior to the delivery of HHV-6A specific gRNAs (6A-gRNAs), we assessed the Cas9 expression in the population. Immunofluorescence staining revealed that not all cells expressed the Cas9 protein despite the selection (Fig. 1A). We therefore decided to quantify the

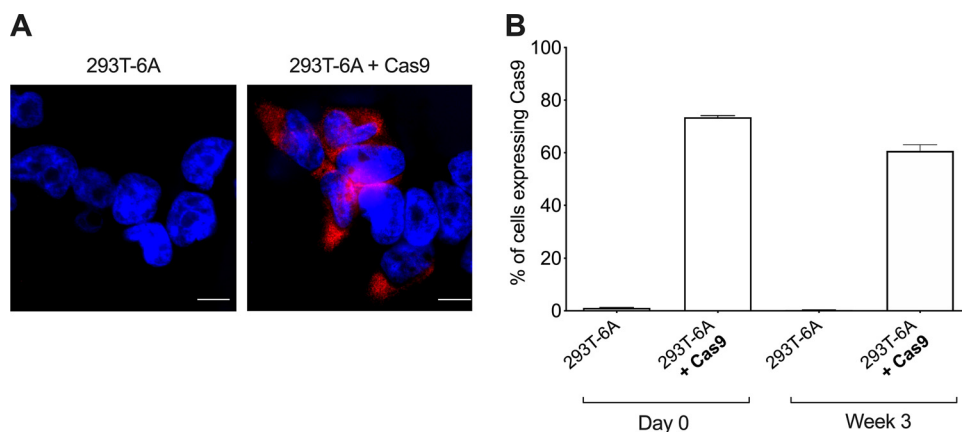


FIG 1 Quantification of Cas9 expression in transduced 293T-6A cells. (A) Cas9 expression was assessed by immunofluorescence using an anti-d-Tag antibody and a secondary Alexa Fluor 568-conjugated antibody (red). Cell nuclei were stained with 4',6-diamidino-2-phenylindole (DAPI) (blue). Untransduced 293T-6A cells were used as a negative control (bar, 10 μ m). (B) Quantification of Cas9 expression was performed by flow cytometry (FACS). Results are shown as means from three independent quantification (one-way ANOVA; $n = 3$; \pm standard error of the mean). Representative FACS plots with gating are shown in Fig. S1 in the supplemental material.

percentage of Cas9-positive cells by flow cytometry. The data revealed that about 70% of the cells expressed Cas9 at various levels. The remaining 30% appeared to be Cas9 negative, suggesting that Cas9 is either quickly downregulated or not expressed upon lentivirus delivery (Fig. 1B, day 0, and see Fig. S1 in the supplemental material). Moreover, the percentage of Cas9-expressing 293T-6A cells decreased over time, indicating that there is a selection pressure against Cas9 expression (Fig. 1B, week 3). Similarly, when we attempted to make Cas9-expressing clones, the production of the protein decreased over time. By the time enough clonal cells were available for the experiments, the percentage of Cas9-positive cells was comparable to that of the original polyclonal population. Therefore, we decided to perform the initial experiments with the polyclonal population.

Removal of integrated HHV-6A genomes using specific gRNAs. To excise the HHV-6A genome, we delivered the second component of the CRISPR/Cas9 system, HHV-6A-specific gRNAs (6A-gRNAs). We designed 10 gRNAs directed against the noncoding region of the DRs at the end of the viral genome (Fig. 2A and Table 1). To deliver multiple gRNAs at once, we used the polycistronic-tRNA-gRNA (PTG) system (56, 57). In this system, the individual gRNAs are interspaced by tRNA sequences and driven by a single U6 promoter (Fig. 2B). Upon transcription, tRNAs are removed by endogenous RNases, resulting in the release of individual gRNAs (Fig. 2B). As a control, we delivered gRNAs targeting another herpesvirus (Marek's disease virus [MDV]) established previously (58).

After transfection of the 293T-6A-Cas9 cells with the 6A-gRNA expression plasmid, we selected the cells using hygromycin and validated the excision by three independent methods. First, we made use of the GFP reporter in the virus genome that is expressed in the cells upon stimulation with phorbol 12-myristate 13-acetate (TPA). FACS analyses revealed a reduction in GFP-expressing cells of about 70% using the 6A-gRNAs, indicating that the HHV-6A genome was successfully removed in most cells (Fig. 3A and Fig. S2). In addition, we assessed the removal of the virus genome by qPCR and observed that the HHV-6A genome copies were also reduced by about 70% compared to the controls (Fig. 3B). Finally, we performed fluorescence *in situ* hybridization (FISH) to visualize the virus genome. In the untransfected and control gRNA-transfected cell, two copies of the integrated virus were readily detected at the ends of metaphase chromosomes using an HHV-6A-specific probe (Fig. 3C, upper images). In contrast, the integrated virus was no longer detectable in most cells transfected with the 6A-gRNAs (Fig. 3C, lower image). We quantified the percentage of cells ($n = 100$) containing the integrated HHV-6 genome, confirming that the virus genome was indeed eliminated in about 70% of them (Fig. 3D). The 70% correspond to the percentage of Cas9-expressing cells, indicating that excision is very efficient provided that the Cas9

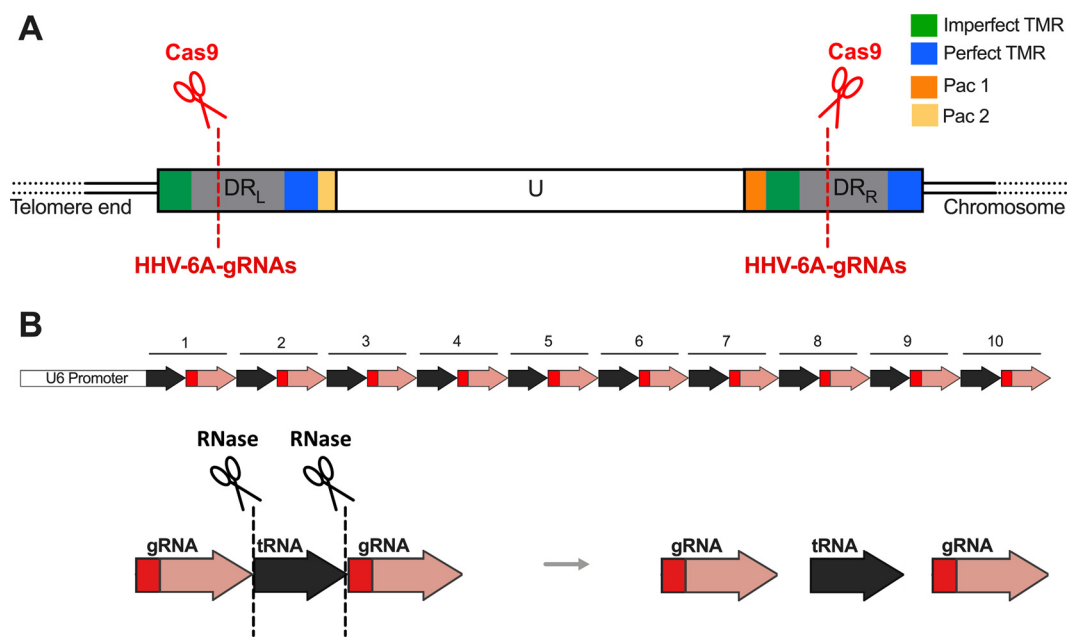


FIG 2 Schematic representation of HHV-6A genome and polycistronic-tRNA-gRNA (PTG) construct. (A) The specific HHV-6A gRNAs designed (red dashed line) were all directed against the noncoding region of the DRs (gray boxes). Driven by the gRNAs, Cas9 protein will excise the HHV-6A genome from the host telomeres. (B) In the PTG construct, the specific HHV-6 gRNAs (red arrows) are interspersed with tRNA sequences (black arrows) and transcribed as a single polycistronic RNA from the U6 promoter. Following transcription, the endogenous cellular RNases will precisely cut out the tRNA sequences, allowing the release of the individual HHV-6A-specific gRNAs.

protein is present. To confirm this, we stained for Cas9 on the FISH slides. Excision occurred only in the presence of Cas9 and the 6A-gRNAs (Fig. 4, panel 4), while the viral genomes were readily detectable in the 30% of cells that did not express Cas9 (Fig. 4, panel 5) as well as in the controls.

To exclude the possibility that the virus reactivates upon excision, we assessed viral gene expression upon transfection of the gRNAs. RT-qPCR revealed that the essential immediate early gene U86 was not detectable (nd) after the excision over time (Fig. 3E). Taken together, our data show that the HHV-6A integrated genome can be successfully removed from chromosomes using the CRISPR/Cas9 system without inducing viral reactivation.

Removal of the integrated HHV-6A genome by transient expression of Cas9.

Considering possible future clinical applications, we decided to assess the removal efficacy upon transient expression of Cas9 to avoid long-term expression of the protein in patient cells. We therefore cloned the PTG cassette into a Cas9 expression plasmid. This vector has the advantage of delivering the two components of the CRISPR/Cas9 system simultaneously, substantially shortening the selection process.

TABLE 1 HHV-6A-specific gRNA sequences (only target sequence shown)

gRNA	Target sequence (5'-3')	PAM ^a (3')	Orientation
gRNA_1	AGGGGCCGGACGTATACGAA	GGG	Antisense
gRNA_2	CTCGTTGCGAAACCGCAACA	GGG	Sense
gRNA_3	AGTCCGTAATAACACCCGAG	GGG	Sense
gRNA_4	GAAACCGAAAGCGTAAAGGG	CGG	Sense
gRNA_5	CTGTCGCTGTCGGAGAACG	TGG	Antisense
gRNA_6	GGAAAGGGGACGTACGGAGA	AGG	Antisense
gRNA_7	GTCGGACCTCGGGTCCGAAG	CGG	Antisense
gRNA_8	CGCCAGACATCGACCGCCGG	AGG	Sense
gRNA_9	GTTGCCGTAGAGGCGTCCGA	GGG	Antisense
gRNA_10	TACCGAATGCAAAAAGTTAA	AGG	Sense

^aPAM, protospacer-adjacent motif.

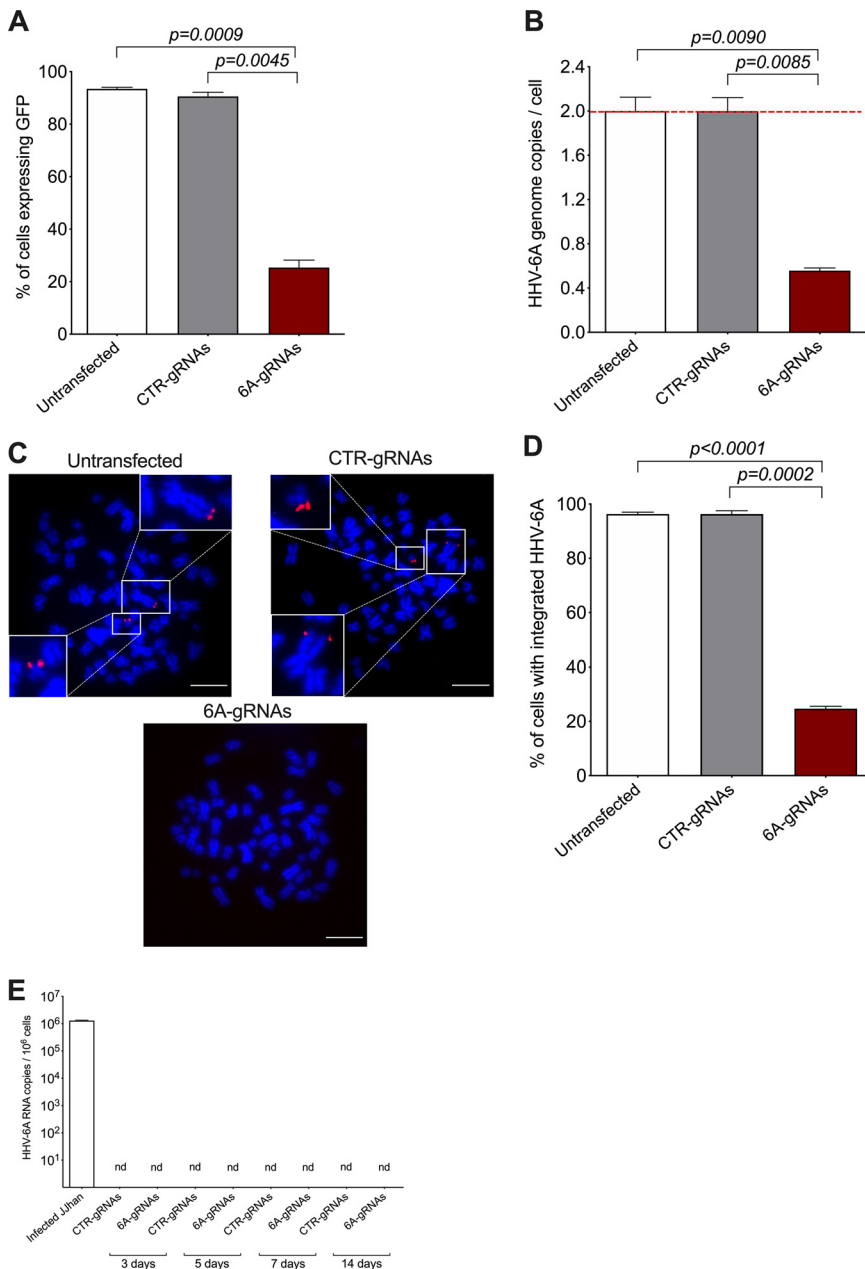


FIG 3 Removal of integrated HHV-6A genome in Cas9-transduced 293T-6A cells. (A) Virus-encoded GFP was detected after TPA stimulation by flow cytometry in untransfected 293T-6A-Cas9 cells or cells transfected with control (CTR) gRNAs or HHV-6A-specific gRNAs. Results are shown as means from three independent experiments (one-way ANOVA; $n = 3$; \pm standard error of the mean). Representative FACS plots including gating strategy are shown in Fig. S2 in the supplemental material. (B) Copy numbers of the HHV-6A U86 gene were detected by qPCR. Results are shown as fold change compared to untransfected 293T-6A-Cas9 cells (red dashed line), which harbor two copies of the integrated virus (one-way ANOVA; $n = 3$; \pm standard error of the mean). (C) Integrated virus was detected by FISH using specific HHV-6A biotin-labeled probes and Cy3-streptavidin antibody (red). Metaphase chromosomes were stained with DAPI (blue). Representative images of indicated conditions are shown in untransfected 293T-6A-Cas9 cells, cells transfected with control gRNAs, and cells transfected with specific HHV-6 gRNAs (bar, 10 μ m). (D) One hundred interphase nuclei were examined for the presence or absence of the integrated virus (one-way ANOVA; $n = 3$; \pm standard error of the mean). (E) Total RNA was extracted at indicated time points after gRNA transfection. The absence of viral transcripts was confirmed for the HHV-6 immediate early gene U86 ($n = 3$; \pm standard error of the mean) by qPCR. As a positive control, RNAs from lytic infected JJhan cells were analyzed. nd, not detected.

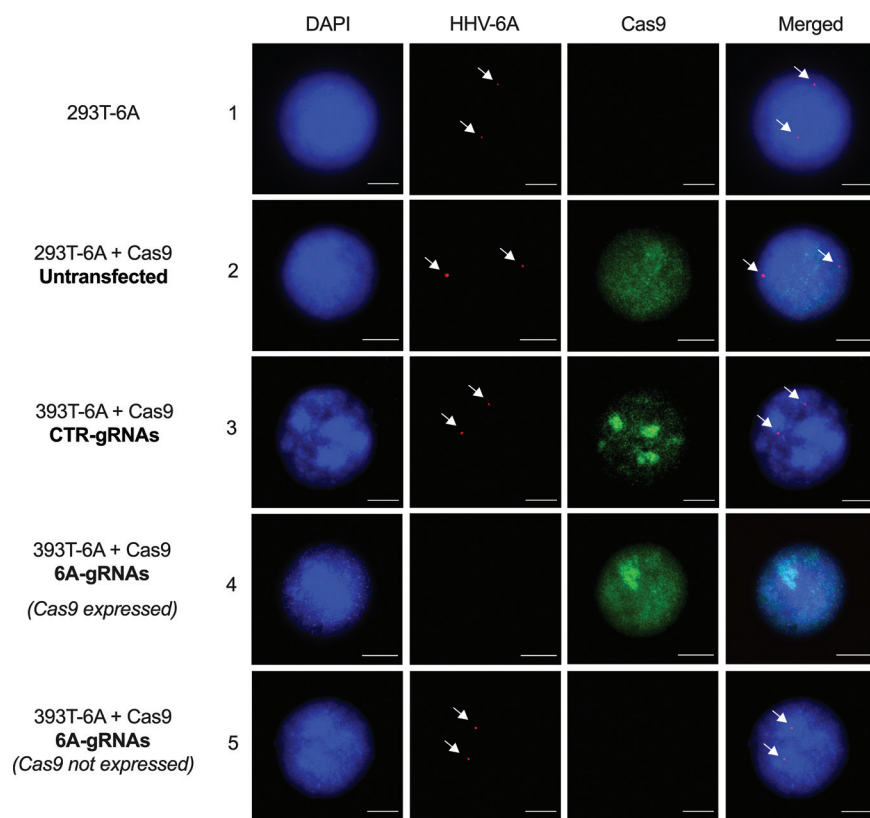


FIG 4 Fluorescence *in situ* hybridization to simultaneously detect integrated HHV-6 and Cas9 protein. Integrated virus was detected by FISH using specific HHV-6A biotin-labeled probes and Cy3-streptavidin antibodies (red). Metaphase chromosomes were stained with DAPI (blue). Cas9 protein was detected with an anti-Cas9 Alexa Fluor 647-conjugated antibody. The arrows indicate the integrated virus genome. Representative images are shown (bar, 10 μ m).

The new plasmid and respective controls were delivered by transient transfection into 293T-6A cells, and the cells were selected with puromycin. As described above, the excision rate was assessed by FACS, qPCR, and FISH. Quantification of the GFP expression upon TPA stimulation revealed a significant reduction of the virus compared to the controls (Fig. 5A and Fig. S4). Quantification of viral genome copies by qPCR confirmed removal of the HHV-6A genome in about 65% of the transfected cells (Fig. 5B). Similarly, FISH images and their quantification revealed that the virus is no longer detectable in most cells transfected with the Cas9 + 6A-gRNAs (Fig. 5C and D). These data highlight that a transient delivery of Cas9 is a good alternative that facilitates the excision of the integrated HHV-6 genome without a prolonged expression of the Cas9 protein.

Removal of integrated HHV-6A genomes from iciHHV-6A patient cell. To determine if the transient excision system also facilitates removal of the virus genome from iciHHV-6A patient cells, we used smooth muscle cells (SMCs). These cells have been immortalized by lentiviral delivery of the simian virus 40 (SV40) large T antigen and harbor 1 copy of the integrated iciHHV-6A genome, as reported in previous studies (54, 55). As described above, iciHHV-6A SMCs were transfected with the plasmid containing Cas9 + 6A-gRNAs and the cells were selected with puromycin. The excision efficiency was subsequently assessed by PCR and FISH. The qPCR data revealed a successful removal of the virus genome in about 57% of the transfected cells (Fig. 6A). These results were confirmed by FISH, showing a significant reduction of the number of cells harboring the integrated virus after the transfection with the Cas9 + 6A-gRNA plasmid (Fig. 6B and C). To exclude the possibility that the virus reactivates upon excision, we assessed viral gene expression upon delivery of the CRISPR/Cas9 system. RT-qPCR revealed that the immediate early gene U86 was not detectable after the excision over time (Fig. 6D).

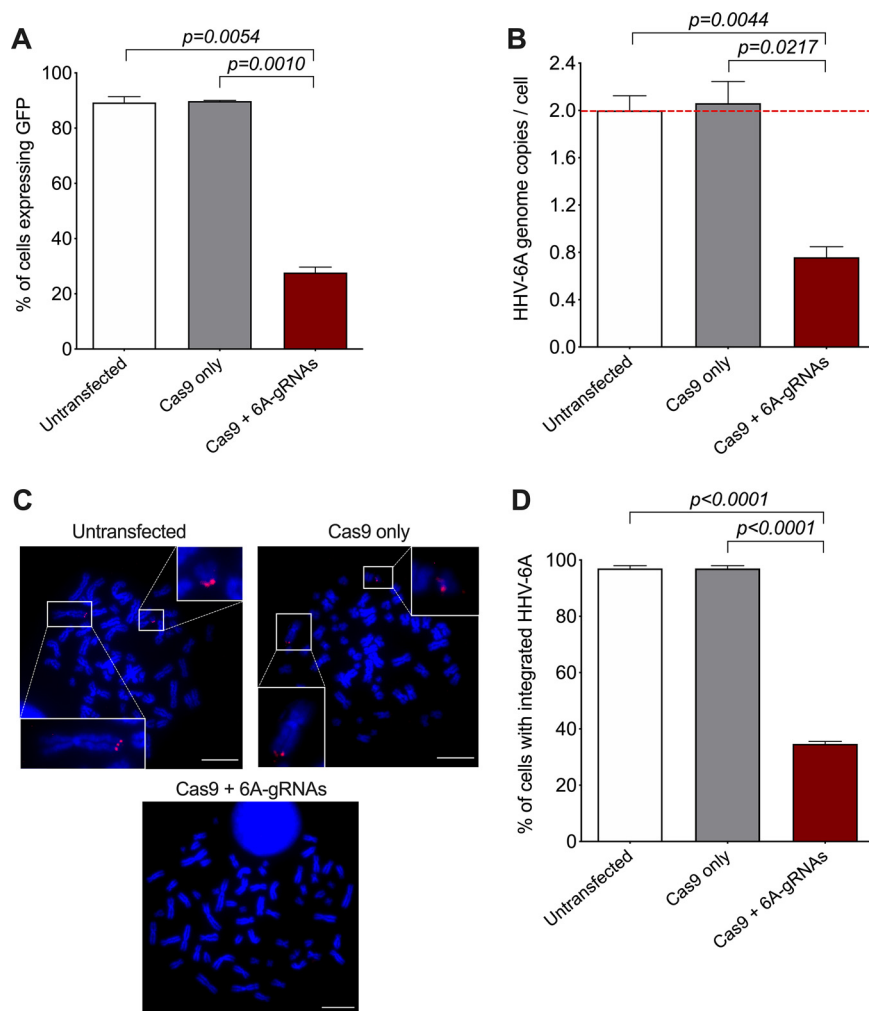


FIG 5 Removal of integrated HHV-6A genome via transient delivery of Cas9 + 6A-gRNAs. (A) Virus-encoded GFP expression was detected after TPA stimulation by flow cytometry in untransfected 293T-6A cells, cells transfected with Cas9 only, and cells transfected with Cas9 + 6A-gRNAs. Results are shown as means from three independent experiments (one-way ANOVA; $n = 3$; \pm standard error of the mean). Representative FACS plots with gating are shown in Fig. S4 in the supplemental material. (B) Copy numbers of HHV-6A U86 gene were detected by qPCR. Results are shown as fold change (red dashed line) compared to untransfected 293T-6A cells, which harbor two copies of the integrated virus (one-way ANOVA; $n = 3$; \pm standard error of the mean). (C) Integrated virus was detected by FISH using specific HHV-6A biotin-labeled probes and Cy3-streptavidin antibody (red). Metaphase chromosomes were stained with DAPI (blue). Representative images of untransfected 293T-6A cells, cells transfected with Cas9 only, and cells transfected with Cas9 + 6A-gRNAs are shown (bar, 10 μ m). (D) One hundred interphase nuclei were examined for the presence or absence of the integrated virus (one-way ANOVA; $n = 3$; \pm standard error of the mean).

Next, we determined if the presence of the remaining integrated virus genomes could be due to reintegration of the virus genome upon excision. Our previous studies demonstrated that the virus is integrated in chromosome 19 in these iciHHV-6A SMCs (55). In cells that still harbored the iciHHV-6A, the virus genome was still detected in chromosome 19, suggesting that the virus genome was not excised in those cells and did not integrate elsewhere upon excision (Fig. S3). Our data demonstrate that the virus genome can be removed from iciHHV-6 patient cells using a transient delivery of Cas9 + 6A-gRNAs.

Removal of integrated HHV-6A genomes by sorting Cas9-expressing cells. We demonstrated that the CRISPR/Cas9 system facilitates the removal of the integrated HHV-6A genome with both stable and transient Cas9 expression. However, a fraction of cells still retained the integrated virus, likely due to the lack of or low level of Cas9

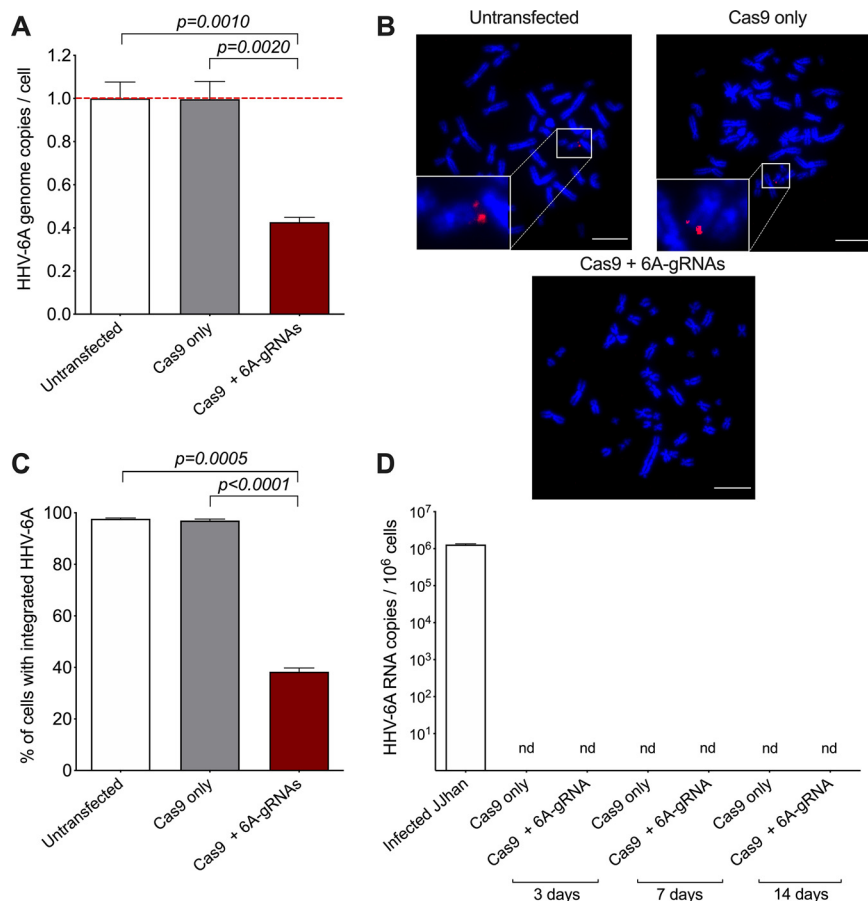


FIG 6 Removal of integrated HHV-6A genome from iciHHV-6A SMCs. (A) Copy numbers of the HHV-6A U86 gene were detected by qPCR. Results are shown as fold change (red dashed line) compared to untransfected iciHHV-6A SMCs, which harbor one copy of the integrated virus (one-way ANOVA; $n = 6$; \pm standard error of the mean). (B) Integrated virus was detected by FISH as described for Fig. 5. Representative images of untransfected iciHHV-6 SMCs, cells transfected with Cas9 only, and cells transfected with Cas9 + 6A-gRNAs are shown (bar, 10 μ m). (C) One hundred interphase nuclei were examined for the presence or absence of the integrated virus (one-way ANOVA; $n = 3$; \pm standard error of the mean). (D) Total RNA was extracted at different time points after transfection. The absence of viral transcripts was confirmed by qPCR for the HHV-6 early gene U86 ($n = 3$; \pm standard error of the mean). As a positive control, RNA from lytic infected JJhan cells was analyzed. nd, not detected.

expression. To overcome this problem, we used a GFP-tagged Cas9 protein to allow isolation of cells expressing a high level of the protein by FACS. We cloned the PTG cassette containing the 6A-gRNAs into a plasmid expressing Cas9-T2A-GFP and transfected the 293T-6A cells with the newly generated plasmid. As a control, we used the plasmid containing only Cas9-T2A-GFP. At 72 h after transfection, we sorted cells with high GFP expression, kept them in culture, and assessed the excision of HHV-6A by qPCR. Results revealed a 55% reduction of the viral genome copies compared to the controls (Fig. 7A). Surprisingly, this approach appeared to be less efficient than our previous approaches, despite the initially high Cas9 levels. To exclude the possibility that some of the detected genome copies account for a viral reactivation after excision and sorting, we performed RT-qPCR. However, no HHV-6A U86 transcripts were detected at different time points after sorting (Fig. 7B).

We therefore decided to track Cas9-T2A-GFP expression in the 293T-6A cells. This revealed a rapid loss of the Cas9 plasmid after sorting. Already after 5 days, the GFP expression was lost in most cells (Fig. 7C). These results suggest that despite the high Cas9 expression early on, the excision is less efficient, likely due to the rapid loss of the Cas9 expression.

Consecutive removal of integrated HHV-6A genomes. To further reduce the number of 293T-6A cells still harboring the integrated HHV-6A, we used two consecutive rounds

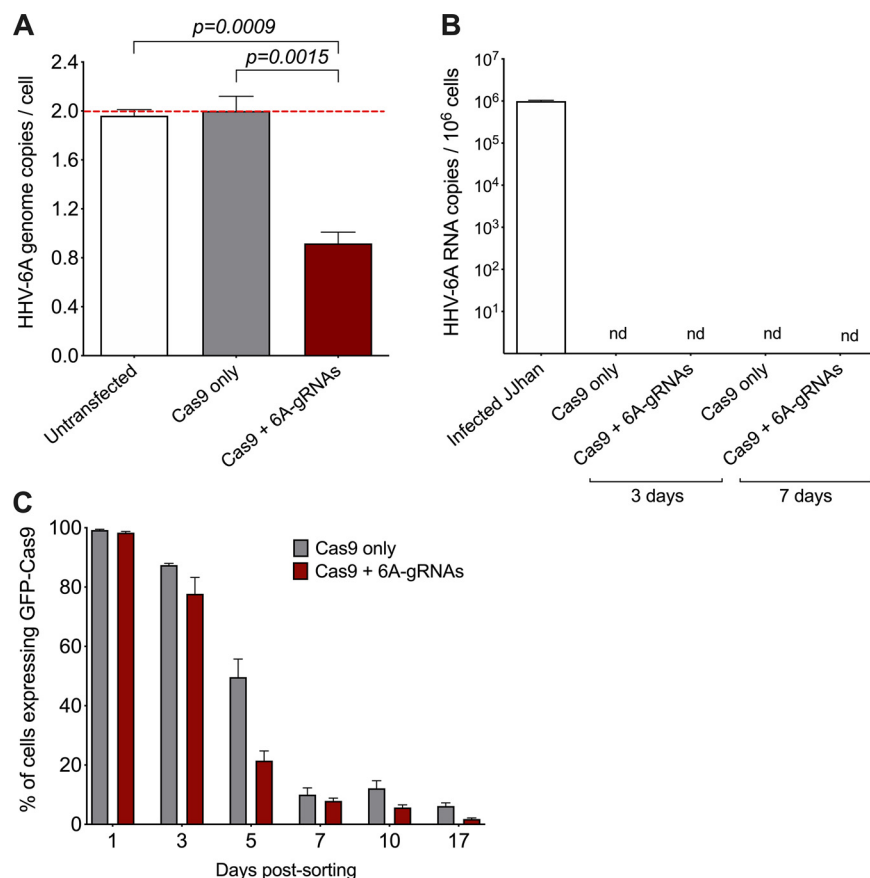


FIG 7 Removal of integrated HHV-6A genome in GFP-Cas9-sorted cells. (A) Copy numbers of the HHV-6A U86 gene were detected by qPCR. Results are shown as fold change (red dashed line) compared to untransfected 293T-6A cells, which harbor two copies of the integrated virus (one-way ANOVA; $n = 3$; \pm standard error of the mean). (B) Total RNA was extracted at different time points after sorting. The absence of viral transcripts was confirmed by qPCR for the HHV-6 early gene U86 ($n = 3$; \pm standard error of the mean). As a positive control, RNA from lytic infected JJhan cells was analyzed. nd, not detected. (C) Expression of the T2A-GFP-pCas9 was followed over time by flow cytometry ($n = 3$; \pm standard error of the mean).

of our transient delivery approach as described above. This aimed at reaching cells in which Cas9 was quickly downregulated or not expressed at all after the first transfection. The second delivery was performed 3 weeks later, when Cas9 expression of the first round had almost disappeared. Quantification of the GFP expression upon TPA stimulation revealed that a second round of the transient delivery eliminated the virus genome in more than 80% of the cells, although the additional reduction was not statistically significant (Fig. 8A). This further reduction was confirmed by the quantification of viral genomes by qPCR (Fig. 8B). These results highlight that two consecutive transient transfections of the CRISPR/Cas9 system can enhance the removal of the integrated HHV-6A genome.

Analysis of the excision sites after the HHV-6A genome removal. Finally, we analyzed the excision sites in our cell populations after the HHV-6A genome removal. As described above, our set of HHV-6A gRNAs targeted the noncoding area in the DRs, between the DR1 and the DR6/7 locus (Fig. 2A and Fig. 9A). Following the successful Cas9-based excision, the full U region and part of the two DRs were removed from the host chromosome (Fig. 9B). After non-homologous end-joining of the two truncated ends, the newly formed junction retained only part of the two original DRs fused together in the host genome (Fig. 9B). To investigate the excision sites, we amplified and sequence the area targeted by the HHV-6 gRNAs (Fig. 9C). Sequencing results revealed the presence of the predicted junction with a high level of heterogeneity at the cut site due to the error-prone non-homologous end-joining mechanism (Fig. 9B). This

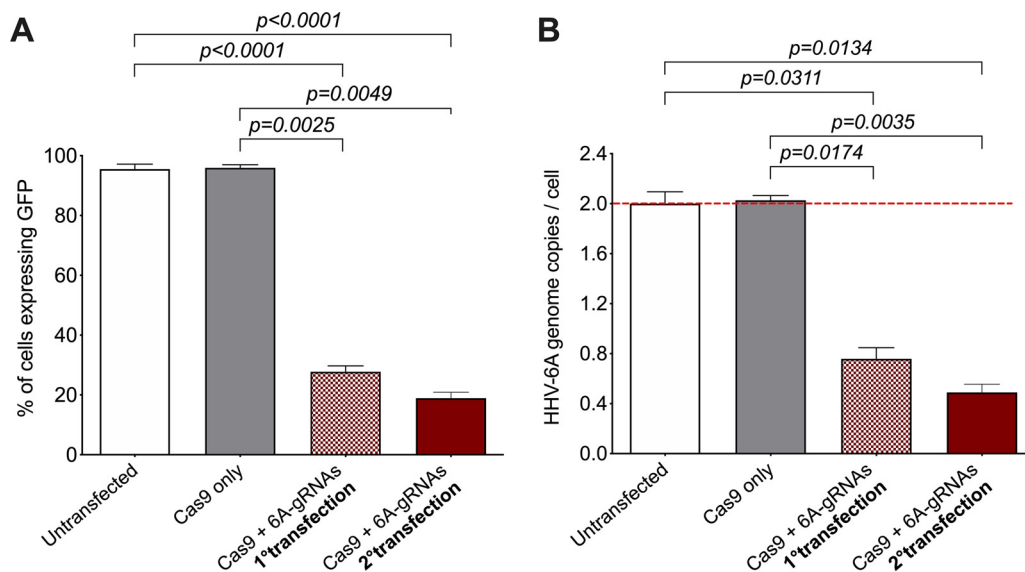


FIG 8 Removal of integrated HHV-6A genome through consecutive transfections. (A) Virus-associated GFP was detected by flow cytometry in untransfected 293T-6A cells, cells transfected with Cas9 only, cells transfected only once with Cas9 + 6A-gRNAs, and cells transfected twice with Cas9 + 6A-gRNAs. Results are shown as means from three independent experiments (one-way ANOVA; $n = 3$; \pm standard error of the mean). (B) Copy numbers of HHV-6A U86 gene were detected by qPCR. Results are shown as fold change compared to untransfected HHV-6 293T cells, which harbor two copies of the integrated virus (one-way ANOVA; $n = 3$; \pm standard error of the mean).

indicated that most cuts occurred at the outermost target sites, highlighting the potential of reducing the number of gRNAs in future studies.

DISCUSSION

In this study, we provide the first proof-of-concept that the integrated HHV-6A genome can be eliminated from the host telomeres using the CRISPR/Cas9 technology. Unlike most herpesviruses, which maintain their genome as circular episomes during latency, HHV-6A/B integrate into the telomere of human chromosomes. Integration makes it impossible to eradicate the virus with pharmacological drugs, which so far only moderately inhibit virus replication and do not prevent latency in the host (10–12).

Over the last several years, the CRISPR/Cas9 system proved to be a powerful tool for genome editing. Recent studies exploited this system to target the latent circular episomes of other herpesviruses, including herpes simplex virus 1 (HSV-1) and cytomegalovirus (CMV), aiming at disrupting single viral genes to abrogate lytic replication and prevent reactivation and/or episome maintenance (59–64). Since HHV-6A/B integrate their genome into the telomeres of latently infected cells, removal of the viral genome with its promoters, genes, and regulatory elements is certainly the best option. This approach could be also applied to other integrated (herpes)viruses.

Here, we designed HHV-6A-specific gRNAs targeting the direct repeats of the virus, to allow the release of the integrated viral genome from the host telomeres. The use of the polycistronic-tRNA-gRNA (Fig. 2A) allowed the delivery of multiple HHV-6-specific gRNAs from a single plasmid (56, 57). This approach is beneficial, as it would allow the removal of a broad range of viral strains without the need for adapting the system to each specific strain. In our initial experiments, we constitutively expressed Cas9 by lentivirus delivery. Upon expression of HHV-6A-specific gRNAs, the virus genome was removed in most cells, providing the first evidence that our system is functional (Fig. 3). Although we observed that the integrated Cas9 gene was slowly downregulated over time, its long-term presence in the cells, and perhaps reemerging expression, could result in an unspecific off-target Cas9 activity. To avoid this, we decided to establish a system that allows transient expression of Cas9 and showed that its expression is lost over time. Our data show how HHV-6A excision can be achieved without constitutive Cas9 expression in both latently

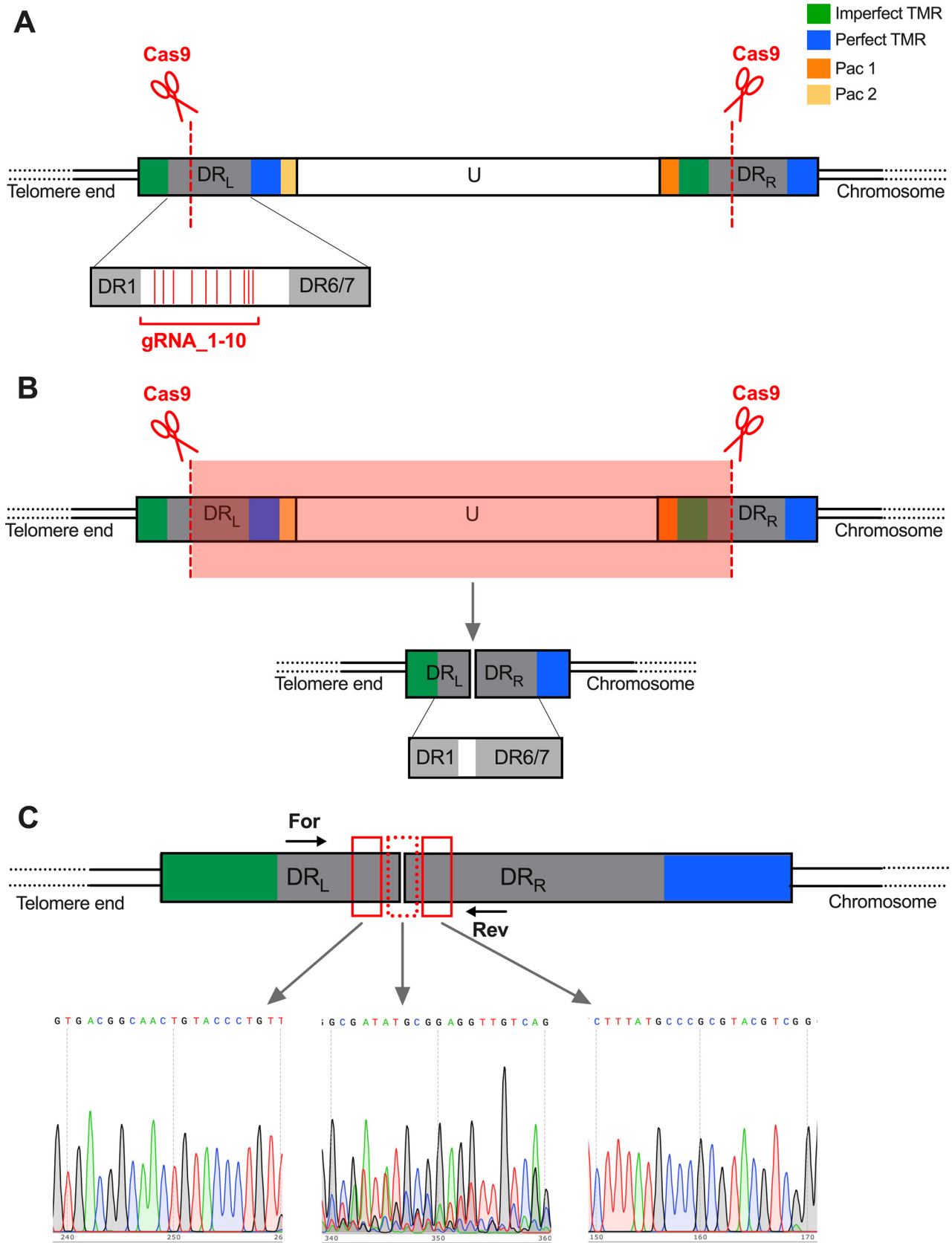


FIG 9 Excision site analysis after Cas9-based removal of the HHV-6A genome. (A) The set of 10 gRNAs targeted a noncoding region in the HHV-6A genome located between DR1 and DR6/7. (B) Following the Cas9 cut in both DRs, the U region, the Pac sequences, and part of the DRs are (Continued on next page)

infected cells generated *in vitro* and iciHHV-6A patient cells. The transient Cas9 expression makes the system more appealing for future possible application.

During the establishment of latency, herpesviruses silence most of their genes to escape the host immune response and persist mostly undetected by the host immune system. This is also true for HHV-6, as its integrated genome is silenced in a compact state and contains a repressive chromatin profile (54). Until now, only a few HHV-6 transcripts have been detected during latency (65–67). The U94 protein has been detected at higher levels during latency than during lytic infection, and its expression has been associated with inhibition of cell migration and increased immune response (68–71). Latent HHV-6 gene expression could therefore influence host cells and the health of the host not only during virus reactivation but also during the latent phase. Supporting an active role of the integrated HHV-6 genome, recent studies highlighted a tissue-specific RNA expression of some viral genes in iciHHV-6 individuals, indicating that certain genes are expressed at some point in time even without complete viral reactivation (65, 66). For instance, specific viral transcripts have been detected in the brain of iciHHV-6A individuals (65), consistent with several studies that associate HHV-6A with various neurological diseases, including multiple sclerosis and Alzheimer's disease (72–78).

It has been hypothesized that the first step of HHV-6A/B reactivation is the release of the virus genome from the chromosomes through a t-loop formation. Recombination between the host telomere and the viral TMR within the DRs would result in the release of a replication-competent circular viral genome with one full-length DR (79–81). Telomere shortening in most somatic cells over time could also play a role in the release and reactivation of the virus, an aspect that should be investigated in the future. Interestingly, our data revealed that the release of the HHV-6A genome after excision does not lead to viral reactivation, as expression of the immediate early U86 gene was not detected in our experiments. These data suggest that the simple viral genome release is *per se* not enough to trigger HHV-6A reactivation. Indeed, the excised virus genome lacks parts of its DRs, retained on the host genome, and does not harbor TMRs at its ends. Therefore, the excised sequence likely will not be able to reconstitute a functional circular viral genome capable of initiating virus replication. On the other hand, the specific circumstances and/or the trigger behind complete viral reactivation is still not fully understood.

Furthermore, our data showed that no reintegration can be detected after the excision of the HHV-6A genome from the host telomeres (see Fig. S3 in the supplemental material). It appears that the mere presence of the excised quiescent HHV-6A genome is not enough to integrate once again. Importantly, following excision with our gRNAs, the released viral genome would lack its TMRs at the end of the virus genome (Fig. 2A). As the viral TMRs have been shown to be required for efficient virus integration, a reintegration event would be rather unlikely (29).

Upon the Cas9-based cleavage of the HHV-6A genome, the U region and large parts of the DRs would be removed. Subsequently, the remaining DR_L and DR_R are fused together by non-homologous end-joining as observed in our PCR analyses (Fig. 9) and retained in the host telomere. The presence of a partial DR without its Pac sequences is also observed upon the release of the virus genome during reactivation via the proposed t-loop model (79, 81). Compared to the unique region, the two DRs remain poorly characterized. Interestingly, DR1 and DR6 loci have been shown to be dispensable for virus replication *in vitro*, as their deletion does not impair virus propagation in T-cell lines (82). As HHV-6A/B specifically integrate into the host telomeres, the excision of the virus genome could affect telomere length. Our sequencing data revealed that the region adjacent

FIG 9 Legend (Continued)

removed from the host genome. Non-homologous end-joining of the two resulting ends results in the generation of an incomplete DR harboring DR1 and DR6/7 from DR_L and DR_R, respectively. (C) Specific primers were used to amplify the excision site in the cell population after Cas9 treatment. The PCR product was the expected size and subsequently sequenced. Sequencing analyses reveal a homogeneous chromatogram profile in the area outside the excision site (left and right chromatograms). The area directly targeted by the gRNA displays a more inhomogeneous profile, in line with error-prone nonhomologous end-joining in the polyclonal cell population (middle chromatogram).

to the excision sites remained intact in the cell population, suggesting that nonhomologous end-joining successfully fuses the two ends while maintaining the original telomere present at the DR_R. In addition, telomere lengthening might also occur in the cells used in this study as they are telomerase positive. Intriguingly, a recent study revealed the presence of long telomere sequences (from 5.0 to 13.3 kbp) between the subtelomeres and the virus genome using a whole-genome optical mapping technology. This implies that HHV-6A/B integration occurs at or near the end of the telomere rather than in proximity to the subtelomeres as previously thought (33). In turn, this suggests that even if no nonhomologous end-joining took place and the DRs eroded, there would still be long telomeres present at the new end of the chromosome.

Taken together, our results highlight that the virus can be successfully eliminated from the telomeres using specific gRNAs against terminal regions of the HHV-6A genome, without triggering viral reactivation. In addition, we showed how a transient Cas9 expression is sufficient to achieve viral excision, without the need of a long-lasting Cas9 expression. Our study provides the first proof-of-concept that the integrated HHV-6A genome can be successfully removed from iciHHV-6 patient cells and latently infected cells generated *in vitro*, providing the basis for future clinical applications. As iciHHV-6 patients harbor the integrated viral genome in every cell of the body, a complete clearance of the virus from these individuals remains impossible. However, our approach could be used to eradicate the virus from specific cell populations or from a subset of cells. For example, this method could be applied to cells used in hematopoietic stem cell transplantations, to clear them of the integrated virus and avoid virus reactivation that can lead to encephalitis, graft rejection, and graft-versus-host disease (GvHD) in immunocompromised patients. Beyond the potential clinical applications, this approach could provide important insights into HHV-6 biology. For example, removal of the virus genome from cells of iciHHV-6 individuals would reveal how the integrated virus genome with its promoters and regulatory elements influences the host cell. This would be a crucial step toward understanding the influence of this virus present in every cell of millions of people.

MATERIALS AND METHODS

Cell lines and virus. HHV-6A-latently infected 293T (293T-6A) cells harboring two copies of the integrated virus genome (strain U1102) were previously generated and described (54, 55). Cells were cultured in Dulbecco's modified Eagle's medium (DMEM) supplemented with 10% fetal bovine serum (FBS; Pan Biotech), 1% penicillin-streptomycin, and 5 μ g/mL Plasmocin (InvivoGen, San Diego, CA, USA). Human smooth muscle cells (SMCs) harboring the integrated iciHHV-6A genome were described previously (54). SMCs were cultured in M199 medium (Pan Biotech) supplemented with 20% FBS (Pan Biotech), 1% penicillin-streptomycin, and 5 μ g/mL Plasmocin (InvivoGen, San Diego, CA, USA). All cells were cultured in a humidified incubator with 5% CO₂.

Lentivirus delivery of Cas9. Cas9 was constitutively expressed upon lentivirus delivery as described previously (83, 84). Briefly, Cas9 lentiviruses were produced by cotransfecting 293T cells with the two packaging vectors PCMV-VSV-G and pCMVDR8.91 and the transfer vector pSicoR-CRISPR-PuroR expressing the *S. pyogenes* Cas9 gene (kindly provided by Robert Jan Lebbink, University Medical Center Utrecht) (60, 85). Lentiviruses were harvested at 48 h post transfection and delivered as described previously (83, 84). Transduction of 293T-6A cells was performed by spin inoculation at 1,200 \times *g* and room temperature for 2 h. After transduction, cells were selected using 1 μ g/mL of puromycin (Invitrogen, Waltham, MA, USA) for 5 days.

Generation of HHV-6A-specific gRNAs. HHV-6A-specific gRNAs (6A-gRNAs) were identified using the GPP sgRNA designer (Broad Institute, <https://portals.broadinstitute.org/gpp/public/analysis-tools/sgma-design>). The gRNAs with the highest specificity for HHV-6A direct repeat (DR) regions were selected. The gRNAs were directed against the noncoding region of the direct repeats, between DR1 and DR6 (Table 1, gRNA sequences, and Fig. 1A). As a control, we used gRNAs specific for the herpesvirus Marek's disease virus (MDV) published previously (58).

To deliver 10 different HHV-6 gRNAs, we used a polycistronic-tRNA-gRNA (PTG) system to produce multiple functional gRNAs from a single U6 promoter as described previously (56, 57). Briefly, each individual gRNA was interspersed with tRNA sequences (Fig. 2B). The gRNA/tRNA cassette was transcribed, and the pre-tRNA sequences were subsequently precisely cleaved at both ends by the endogenous RNases, releasing the 10 individual HHV-6A gRNAs (86–89) (Fig. 2B). The designed U6-PTG.sg6A cassette, harboring the 6A-gRNAs and the tRNA sequences under the control of the U6 promoter, was synthesized by GeneArt Gene Service (BioPark, Regensburg, Germany).

Generation and delivery of gRNAs and Cas9 + gRNA vectors. The U6-PTG.sg6A cassette was first cloned into the PLKO5.sgRNA.EFS.PAC vector (Addgene catalog no. 57825) (90) containing a hygromycin selection cassette instead of puromycin as described previously (58). The newly generated plasmid PLKO5-PTG.sg6A

TABLE 2 Annealed oligonucleotides for the insertion of BsrGI sites into the U6-PTG.sg6A cassette

Oligos sequences	Used restriction sites	Inserted restriction sites
5' – AATTCGATCTGTACATTTCAG – 3' 3'– GCTAGACATGTAAGTCTTAA – 5'	EcoRI	BsrGI
5' – GACCCGACTTGTACATCTAGG – 3' 3'– GGCTGAACATGTAGATCTTAA – 5'	PpuMI	BsrGI

was used to deliver the 6A-gRNAs into the 293T-6A-Cas9 cells. Transfection was performed using the polycation polyethylenimine (PEI), and transfected cells were selected using 400 $\mu\text{g}/\text{mL}$ hygromycin for 7 days.

To generate a plasmid that expresses both Cas9 and the 6A-gRNAs, the U6-PTG.sg6A cassette of the PLKO5.PTG.sg6A plasmid was cloned into the pSicoR-CRISPR-PuroR Cas9 plasmid. First, EcoRI and PpuMI sites were used to insert two new BsrGI restriction sites at the extremity of the U6-PTG.sg6A cassette using a complementary oligonucleotide annealing approach (oligonucleotides used are shown in Table 2). The cassette was then cloned into the pSicoR-CRISPR-PuroR Cas9 plasmid using the new BsrGI restriction sites. Correct insertion and orientation of the cassette were confirmed by restriction fragment length polymorphism (RFLP) and Sanger sequencing (LGC Genomics, Berlin, Germany). The new final plasmid pCas9-PTG.sg6A was delivered into 293T-6A cells and iciHHV-6A SMCs. Transfection of 293T-6A cells was performed using PEI, while iciHHV-6A SMCs were transfected using X-fect single shots (TaKaRa Bio, Kusatsu, Japan) according to the manufacturer's guidelines. Cells were selected using 1 $\mu\text{g}/\text{mL}$ of puromycin (Invitrogen, Waltham, MA, USA) for 5 days.

To visualize and sort Cas9-expressing cells, we cloned the U6-PTG.sg6A cassette into the vector pSpCas9(BB)-2A-GFP (Addgene catalog no. 48138), containing GFP fused to Cas9 via a T2A ribosome skipping motif (91) using BsrGI. Correct insertion and orientation of the cassette were confirmed by RFLP and Sanger sequencing (LGC Genomics, Berlin, Germany). Transfection of the new plasmid pCas9.GFP-PTG.sg6A into 293T-6A cells was performed using PEI. At 72 h after transfection, cells expressing high levels of Cas9-T2A_GFP were sorted using a FACS Aria III cell sorter (BD Biosciences).

Cas9 protein detection by flow cytometry and immunofluorescence. To determine which cells express Cas9, we stained and analyzed them by FACS. Cells were fixed with 4% paraformaldehyde (PFA) (Sigma-Aldrich, St. Louis, MO, USA) for 30 min. Permeabilization was achieved with 0.3% Triton X-100 (Merck, Darmstadt, Germany) in phosphate-buffered saline (PBS) for 10 min, and blocking was performed with 10% bovine serum albumin (BSA) (AppliChem, Darmstadt, Germany) plus 0.3% Triton X-100 in PBS for 45 min. Cas9 was detected using the mouse anti-Cas9 monoclonal antibody (MAb) (7A9-3A3) conjugated with Alexa Fluor 647 (catalog no. 48796; Cell Signaling, Danvers, MA, USA) at a 1:200 dilution in PBS. The Cas9-Alexa 647 signal was detected and quantified using a CytoFlex S instrument (Beckman Coulter, Brea, CA, USA). Results were analyzed using the FlowJo software.

In addition, Cas9 protein expression was detected by immunofluorescence. Cells were seeded on pre-coated slides in 24-well plates. Cells were fixed, permeabilized, and blocked as described above for the FACS staining. Cas9 was detected by using the anti-d-Tag mouse MAb (ABM, Richmond, BC, Canada) at a 1:250 dilution in PBS to detect the synthetic peptide DYKDDDDK in the Cas9 protein. The secondary Alexa Fluor 568-conjugated anti-mouse antibody (Invitrogen, Waltham, MA, USA) was used at a 1:2,000 dilution in PBS. Images were acquired with a Zeiss M1 microscope using a 100 \times objective and the AxioVision software (Carl Zeiss, Inc.). Images were analyzed using ImageJ (<https://imagej.nih.gov/ij/>) and its specific processing package Fiji (<https://imagej.net/Fiji>).

Detection of the virus-encoded GFP upon stimulation. 293T-6A cells were stimulated with phorbol 12-myristate 13-acetate (TPA; Sigma-Aldrich) (1 $\mu\text{g}/\text{mL}$) for 24 h to induce the expression of the GFP under the control of the HCMV major intermediate early promoter as described previously (54). The GFP signal was detected and quantified by flow cytometry using a CytoFlex S Instrument (Beckman Coulter, Brea, CA, USA). Results were analyzed using the FlowJo software.

Quantification of the HHV-6 genome by qPCR. DNA was isolated from samples using the Zymos Quick-DNA viral kit following the manufacturer's instructions. qPCR was performed as described previously using primers and probes specific for the HHV-6A U86 and the cellular $\beta_2\text{M}$ gene using the SensiFAST master mix (Bioline, Memphis, TN, USA) (29, 35). The viral genome copies (U86) were subsequently normalized against the cellular $\beta_2\text{M}$ gene. The qPCRs were performed using an ABI 7500 Fast system (Applied Biosystems, Waltham, MA, USA) (Fig. 3 and 5) or a qTOWER³ G qPCR (Analytik Jena, Jena, Germany) (Fig. 6, 7, and 8).

Detection of HHV-6A immediate early gene expression. To assess HHV-6A reactivation, we assessed the expression of an immediate early gene (U86) that is expressed during virus replication and reactivation. Total RNA of 293T-6A and iciHHV-6A SMCs upon virus genome excision was extracted using the RNeasy Plus minikit (Qiagen, Hilden, Germany) according to the manufacturer's instructions. Potential carry-over of DNA contamination was removed using the RQ1 DNase (Promega, Madison, WI, USA) according to

TABLE 3 Primers for the amplification of the excision junction region

Primer	Sequence
Forward	5'-AAAGAGTACGTCCTCC-3'
Reverse	5'-ACGTCACGTGAAAAATGTTT-3'

the manufacturer's instructions. cDNA was generated using the high-capacity cDNA reverse transcription kit (Applied Biosystems, Waltham, MA, USA). qPCR was performed as described above.

Detection of HHV-6A genomes by FISH. The integrated HHV-6A genome was detected by fluorescence *in situ* hybridization (FISH) as described previously (29, 92, 93) with the following modifications. Briefly, HHV-6A probes were generated using the HHV-6A bacterial artificial chromosome (BAC) (U1102 strain) and labeled using High-Prime biotin (Sigma-Aldrich, St. Louis, MO, USA). Detection of the HHV-6A probe signal was achieved using Cy3-streptavidin (1:1,000; Roche, Basel, Switzerland). A chromosome 19-specific probe was generated using High-Prime digoxigenin (DIG) (Sigma-Aldrich, St. Louis, MO, USA) and a chromosome-specific BAC clone (RPC1-11; Source BioScience, Nottingham, England) as described previously (93). Detection of chromosome probe signal was achieved using anti-DIG fluorescein isothiocyanate (FITC) Fab fragments (1:200; Roche, Basel, Switzerland). To obtain an adequate number of metaphases, 293T-6A cells were treated with colcemid for 5 h, while iHHV-6 SMCs were treated with colcemid for 16 h prior to sample preparation.

To detect Cas9 in HHV-6A FISH samples, staining of the Cas9 protein was performed with the mouse anti-Cas9 MAb (7A9-3A3) conjugated with Alexa Fluor 647 (1:200; catalog no. 48796; Cell Signaling, Danvers, MA, USA). Images were acquired with a Zeiss M1 microscope using a 100× objective and AxioVision software (Carl Zeiss, Inc.). Images were analyzed using ImageJ (<https://imagej.nih.gov/ij/>) and its specific processing package Fiji (<https://imagej.net/Fiji>).

Sequencing of the excision junction after HHV-6 genome removal. DNA was isolated from samples using the Zymos Quick-DNA viral kit following the manufacturer's instructions. The primers listed in Table 3, located outside the 6A-gRNA target sequences, were used to amplify the region of the excision junction. PCR amplification was performed using the PrimeSTAR GXL DNA polymerase (TaKaRa Bio, Kusatsu, Japan) following the manufacturer's instructions. The PCR products were purified using the high-yield PCR/gel extraction kit (Süd-Laborbedarf GmbH, Gauting, Germany). The purified PCR products were sequenced by Sanger sequencing (LGC Genomics, Berlin, Germany), and results were analyzed using SnapGene software (<https://www.snapgene.com/>). The HHV-6A strain U1102 genome was used as a reference genome for the analysis.

Statistical analysis. All statistical analyses were performed using GraphPad Prism. One-way analysis of variance (ANOVA) was performed, with Geisser-Greenhouse correction and Tukey's multiple-comparison test.

Ethics approval and consent to participate. Ethics approval and consent to participate are not applicable.

Data availability. The data sets supporting the conclusions of this article are included within the article and its supplemental material.

SUPPLEMENTAL MATERIAL

Supplemental material is available online only.

SUPPLEMENTAL FILE 1, PDF file, 0.6 MB.

ACKNOWLEDGMENTS

We are grateful to Ann Reum and Yvonne Weber for their technical assistance.

G.A. and B.B.K. designed the experiments; G.A. performed the experiments and analyzed the data; D.J.W. contributed with experimental support and plasmid design; L.F. provided crucial reagents and resources; G.A. and B.B.K. wrote the article; B.B.K. acquired funding. All authors edited and approved the article.

This study was supported by the European Research Council (2) grant Stg 677673 and CoG 101087480, and the Deutsche Forschungsgemeinschaft (DFG) grant KA 3492/6-1 awarded to B.B.K.

We declare that we have no competing interests.

REFERENCES

- Braun DK, Dominguez G, Pellett PE. 1997. Human herpesvirus 6. *Clin Microbiol Rev* 10:521–567. <https://doi.org/10.1128/CMR.10.3.521>.
- De Bolle L, Naesens L, De Clercq E. 2005. Update on human herpesvirus 6 biology, clinical features, and therapy. *Clin Microbiol Rev* 18:217–245. <https://doi.org/10.1128/CMR.18.1.217-245.2005>.
- Agut H, Bonnafous P, Gautheret-Dejean A. 2015. Laboratory and clinical aspects of human herpesvirus 6 infections. *Clin Microbiol Rev* 28:313–335. <https://doi.org/10.1128/CMR.00122-14>.
- Isegawa Y, Mukai T, Nakano K, Kagawa M, Chen J, Mori Y, Sunagawa T, Kawanishi K, Sashihara J, Hata A, Zou P, Kosuge H, Yamanishi K. 1999. Comparison of the complete DNA sequences of human herpesvirus 6 variants A and B. *J Virol* 73:8053–8063. <https://doi.org/10.1128/JVI.73.10.8053-8063.1999>.
- Yamanishi K, Okuno T, Shiraki K, Takahashi M, Kondo T, Asano Y, Kurata T. 1988. Identification of human herpesvirus-6 as a causal agent for exanthem subitum. *Lancet* i:1065–1067. [https://doi.org/10.1016/s0140-6736\(88\)91893-4](https://doi.org/10.1016/s0140-6736(88)91893-4).
- Tesini BL, Epstein LG, Caserta MT. 2014. Clinical impact of primary infection with roseoloviruses. *Curr Opin Virol* 9:91–96. <https://doi.org/10.1016/j.coviro.2014.09.013>.

7. Mohammadpour Touserani F, Gainza-Lein M, Jafarpour S, Brinegar K, Kapur K, Lodenkemper T. 2017. HHV-6 and seizure: a systematic review and meta-analysis. *J Med Virol* 89:161–169. <https://doi.org/10.1002/jmv.24594>.
8. Kondo K, Kondo T, Okuno T, Takahashi M, Yamanishi K. 1991. Latent human herpesvirus 6 infection of human monocytes/macrophages. *J Gen Virol* 72:1401–1408. <https://doi.org/10.1099/0022-1317-72-6-1401>.
9. Luppi M, Marasca R, Barozzi P, Ferrari S, Ceccherini-Nelli L, Batoni G, Merelli E, Torelli G. 1993. Three cases of human herpesvirus-6 latent infection: integration of viral genome in peripheral blood mononuclear cell DNA. *J Med Virol* 40:44–52. <https://doi.org/10.1002/jmv.1890400110>.
10. Nacheva EP, Ward KN, Brazma D, Virgili A, Howard J, Leong HN, Clark DA. 2008. Human herpesvirus 6 integrates within telomeric regions as evidenced by five different chromosomal sites. *J Med Virol* 80:1952–1958. <https://doi.org/10.1002/jmv.21299>.
11. Arbuckle JH, Medveczky MM, Luka J, Hadley SH, Luegmayr A, Ablashi D, Lund TC, Tolar J, De Meirleir K, Montoya JG, Komaroff AL, Ambros PF, Medveczky PG. 2010. The latent human herpesvirus-6A genome specifically integrates in telomeres of human chromosomes in vivo and in vitro. *Proc Natl Acad Sci U S A* 107:5563–5568. <https://doi.org/10.1073/pnas.0913586107>.
12. Osterrieder N, Wallaschek N, Kaufer BB. 2014. Herpesvirus genome integration into telomeric repeats of host cell chromosomes. *Annu Rev Virol* 1:215–235. <https://doi.org/10.1146/annurev-virology-031413-085422>.
13. Kaufer BB, Flamand L. 2014. Chromosomally integrated HHV-6: impact on virus, cell and organismal biology. *Curr Opin Virol* 9:111–118. <https://doi.org/10.1016/j.coviro.2014.09.010>.
14. Tanaka-Taya K, Sashihara J, Kurahashi H, Amo K, Miyagawa H, Kondo K, Okada S, Yamanishi K. 2004. Human herpesvirus 6 (HHV-6) is transmitted from parent to child in an integrated form and characterization of cases with chromosomally integrated HHV-6 DNA. *J Med Virol* 73:465–473. <https://doi.org/10.1002/jmv.20113>.
15. Daibata M, Taguchi T, Nemoto Y, Taguchi H, Miyoshi I. 1999. Inheritance of chromosomally integrated human herpesvirus 6 DNA. *Blood* 94:1545–1549. <https://doi.org/10.1182/blood.V94.5.1545>.
16. Endo A, Watanabe K, Ohye T, Suzuki K, Matsubara T, Shimizu N, Kurahashi H, Yoshikawa T, Katano H, Inoue N, Imai K, Takagi M, Morio T, Mizutani S. 2014. Molecular and virological evidence of viral activation from chromosomally integrated human herpesvirus 6A in a patient with X-linked severe combined immunodeficiency. *Clin Infect Dis* 59:545–548. <https://doi.org/10.1093/cid/ciu323>.
17. Phan TL, Carlin K, Ljungman P, Politikos I, Boussiotis V, Boeckh M, Shaffer ML, Zerr DM. 2018. Human herpesvirus-6B reactivation is a risk factor for grades II to IV acute graft-versus-host disease after hematopoietic stem cell transplantation: a systematic review and meta-analysis. *Biol Blood Marrow Transplant* 24:2324–2336. <https://doi.org/10.1016/j.bbmt.2018.04.021>.
18. Gravel A, Dubuc I, Morissette G, Sedlak RH, Jerome KR, Flamand L. 2015. Inherited chromosomally integrated human herpesvirus 6 as a predisposing risk factor for the development of angina pectoris. *Proc Natl Acad Sci U S A* 112:8058–8063. <https://doi.org/10.1073/pnas.1502741112>.
19. Kühl U, Lassner D, Wallaschek N, Gross UM, Krueger GR, Seeberger B, Kaufer BB, Escher F, Poller W, Schultheiss HP. 2015. Chromosomally integrated human herpesvirus 6 in heart failure: prevalence and treatment. *Eur J Heart Fail* 17:9–19. <https://doi.org/10.1002/ejhf.194>.
20. Wang Y, Wang D, Tao X. 2021. Human herpesvirus 6B encephalitis in a liver transplant recipient: a case report and review of the literature. *Transpl Infect Dis* 23:e13403. <https://doi.org/10.1111/tid.13403>.
21. Hill JA, Magaret AS, Hall-Sedlak R, Mikhaylova A, Huang ML, Sandmaier BM, Hansen JA, Jerome KR, Zerr DM, Boeckh M. 2017. Outcomes of hematopoietic cell transplantation using donors or recipients with inherited chromosomally integrated HHV-6. *Blood* 130:1062–1069. <https://doi.org/10.1182/blood-2017-03-775759>.
22. Gompels UA, Nicholas J, Lawrence G, Jones M, Thomson BJ, Martin ME, Efsthathiou S, Craxton M, Macaulay HA. 1995. The DNA sequence of human herpesvirus-6: structure, coding content, and genome evolution. *Virology* 209:29–51. <https://doi.org/10.1006/viro.1995.1228>.
23. Martin ME, Thomson BJ, Honess RW, Craxton MA, Gompels UA, Liu MY, Littler E, Arrand JR, Teo I, Jones MD. 1991. The genome of human herpesvirus 6: maps of unit-length and concatemeric genomes for nine restriction endonucleases. *J Gen Virol* 72:157–168. <https://doi.org/10.1099/0022-1317-72-1-157>.
24. Dominguez G, Dambaugh TR, Stamey FR, Dewhurst S, Inoue N, Pellett PE. 1999. Human herpesvirus 6B genome sequence: coding content and comparison with human herpesvirus 6A. *J Virol* 73:8040–8052. <https://doi.org/10.1128/JVI.73.10.8040-8052.1999>.
25. Thomson BJ, Dewhurst S, Gray D. 1994. Structure and heterogeneity of the a sequences of human herpesvirus 6 strain variants U1102 and Z29 and identification of human telomeric repeat sequences at the genomic termini. *J Virol* 68:3007–3014. <https://doi.org/10.1128/JVI.68.5.3007-3014.1994>.
26. Gompels UA, Macaulay HA. 1995. Characterization of human telomeric repeat sequences from human herpesvirus 6 and relationship to replication. *J Gen Virol* 76:451–458. <https://doi.org/10.1099/0022-1317-76-2-451>.
27. Kishi M, Harada H, Takahashi M, Tanaka A, Hayashi M, Nonoyama M, Josephs SF, Buchbinder A, Schachter F, Ablashi DV. 1988. A repeat sequence, GGGTTA, is shared by DNA of human herpesvirus 6 and Marek's disease virus. *J Virol* 62:4824–4827. <https://doi.org/10.1128/JVI.62.12.4824-4827.1988>.
28. Achour A, Malet I, Deback C, Bonnafeous P, Boutolleau D, Gautheret-Dejean A, Agut H. 2009. Length variability of telomeric repeat sequences of human herpesvirus 6 DNA. *J Virol Methods* 159:127–130. <https://doi.org/10.1016/j.jviromet.2009.03.002>.
29. Wallaschek N, Sanyal A, Pirzer F, Gravel A, Mori Y, Flamand L, Kaufer BB. 2016. The telomeric repeats of human herpesvirus 6A (HHV-6A) are required for efficient virus integration. *PLoS Pathog* 12:e1005666. <https://doi.org/10.1371/journal.ppat.1005666>.
30. Arbuckle JH, Pantry SN, Medveczky MM, Prichett J, Loomis KS, Ablashi D, Medveczky PG. 2013. Mapping the telomere integrated genome of human herpesvirus 6A and 6B. *Virology* 442:3–11. <https://doi.org/10.1016/j.viro.2013.03.030>.
31. Arbuckle JH, Medveczky PG. 2011. The molecular biology of human herpesvirus-6 latency and telomere integration. *Microbes Infect* 13:731–741. <https://doi.org/10.1016/j.micinf.2011.03.006>.
32. Ohye T, Inagaki H, Ihira M, Higashimoto Y, Kato K, Oikawa J, Yagasaki H, Niizuma T, Takahashi Y, Kojima S, Yoshikawa T, Kurahashi H. 2014. Dual roles for the telomeric repeats in chromosomally integrated human herpesvirus-6. *Sci Rep* 4:4559. <https://doi.org/10.1038/srep04559>.
33. Wight DJ, Aimola G, Aswad A, Jill Lai CY, Bahamon C, Hong K, Hill JA, Kaufer BB. 2020. Unbiased optical mapping of telomere-integrated endogenous human herpesvirus 6. *Proc Natl Acad Sci U S A* 117:31410–31416. <https://doi.org/10.1073/pnas.2011872117>.
34. Wallaschek N, Gravel A, Flamand L, Kaufer BB. 2016. The putative U94 integrase is dispensable for human herpesvirus 6 (HHV-6) chromosomal integration. *J Gen Virol* 97:1899–1903. <https://doi.org/10.1099/jgv.0.000502>.
35. Wight DJ, Wallaschek N, Sanyal A, Weller SK, Flamand L, Kaufer BB. 2018. Viral proteins U41 and U70 of human herpesvirus 6A are dispensable for telomere integration. *Viruses* 10:656. <https://doi.org/10.3390/v10110656>.
36. Collin V, Gravel A, Kaufer BB, Flamand L. 2018. Role of PML-nuclear bodies in human herpesvirus 6A and 6B genome integration. *bioRxiv*. <https://doi.org/10.1101/413575>.
37. Gilbert-Girard S, Gravel A, Collin V, Wight DJ, Kaufer BB, Lazerini-Denchi E, Flamand L. 2020. Role for the shelterin protein TRF2 in human herpesvirus 6A/B chromosomal integration. *PLoS Pathog* 16:e1008496. <https://doi.org/10.1371/journal.ppat.1008496>.
38. Gravel A, Gosselin J, Flamand L. 2002. Human herpesvirus 6 immediate-early 1 protein is a sumoylated nuclear phosphoprotein colocalizing with promyelocytic leukemia protein-associated nuclear bodies. *J Biol Chem* 277:19679–19687. <https://doi.org/10.1074/jbc.M200836200>.
39. Aimola G, Beythien G, Aswad A, Kaufer BB. 2020. Current understanding of human herpesvirus 6 (HHV-6) chromosomal integration. *Antiviral Res* 176:104720. <https://doi.org/10.1016/j.antiviral.2020.104720>.
40. Horvath P, Barrangou R. 2010. CRISPR/Cas, the immune system of bacteria and archaea. *Science* 327:167–170. <https://doi.org/10.1126/science.1179555>.
41. Wiedenheft B, Sternberg SH, Doudna JA. 2012. RNA-guided genetic silencing systems in bacteria and archaea. *Nature* 482:331–338. <https://doi.org/10.1038/nature10886>.
42. Brouns SJ, Jore MM, Lundgren M, Westra ER, Slijkhuys RJ, Snijders AP, Dickman MJ, Makarova KS, Koonin EV, van der Oost J. 2008. Small CRISPR RNAs guide antiviral defense in prokaryotes. *Science* 321:960–964. <https://doi.org/10.1126/science.1159689>.
43. Barrangou R, Fremaux C, Deveau H, Richards M, Boyaval P, Moineau S, Romero DA, Horvath P. 2007. CRISPR provides acquired resistance against viruses in prokaryotes. *Science* 315:1709–1712. <https://doi.org/10.1126/science.1138140>.
44. Makarova KS, Wolf YI, Alkhnbashi OS, Costa F, Shah SA, Saunders SJ, Barrangou R, Brouns SJ, Charpentier E, Haft DH, Horvath P, Moineau S, Mojica FJ, Terns RM, Terns MP, White MF, Yakunin AF, Garrett RA, van der Oost J, Backofen R, Koonin EV. 2015. An updated evolutionary classification of CRISPR-Cas systems. *Nat Rev Microbiol* 13:722–736. <https://doi.org/10.1038/nrmicro3569>.

45. Hsu PD, Lander ES, Zhang F. 2014. Development and applications of CRISPR-Cas9 for genome engineering. *Cell* 157:1262–1278. <https://doi.org/10.1016/j.cell.2014.05.010>.
46. Jinek M, Chylinski K, Fonfara I, Hauer M, Doudna JA, Charpentier E. 2012. A programmable dual-RNA-guided DNA endonuclease in adaptive bacterial immunity. *Science* 337:816–821. <https://doi.org/10.1126/science.1225829>.
47. Mali P, Yang L, Esvelt KM, Aach J, Guell M, DiCarlo JE, Norville JE, Church GM. 2013. RNA-guided human genome engineering via Cas9. *Science* 339:823–826. <https://doi.org/10.1126/science.1232033>.
48. Wright AV, Nuñez JK, Doudna JA. 2016. Biology and applications of CRISPR systems: harnessing nature's toolbox for genome engineering. *Cell* 164:29–44. <https://doi.org/10.1016/j.cell.2015.12.035>.
49. Hale CR, Zhao P, Olson S, Duff MO, Graveley BR, Wells L, Terns RM, Terns MP. 2009. RNA-guided RNA cleavage by a CRISPR RNA-Cas protein complex. *Cell* 139:945–956. <https://doi.org/10.1016/j.cell.2009.07.040>.
50. Sander JD, Joung JK. 2014. CRISPR-Cas systems for editing, regulating and targeting genomes. *Nat Biotechnol* 32:347–355. <https://doi.org/10.1038/nbt.2842>.
51. Mali P, Esvelt KM, Church GM. 2013. Cas9 as a versatile tool for engineering biology. *Nat Methods* 10:957–963. <https://doi.org/10.1038/nmeth.2649>.
52. Doudna JA, Charpentier E. 2014. Genome editing. The new frontier of genome engineering with CRISPR-Cas9. *Science* 346:1258096. <https://doi.org/10.1126/science.1258096>.
53. Cong L, Ran FA, Cox D, Lin S, Barretto R, Habib N, Hsu PD, Wu X, Jiang W, Marraffini LA, Zhang F. 2013. Multiplex genome engineering using CRISPR/Cas systems. *Science* 339:819–823. <https://doi.org/10.1126/science.1231143>.
54. Saviola AJ, Zimmermann C, Mariani MP, Signorelli SA, Gerrard DL, Boyd JR, Wight DJ, Morrisette G, Gravel A, Dubuc I, Flamand L, Kaufer BB, Fritze S. 2019. Chromatin profiles of chromosomally integrated human herpesvirus-6A. *Front Microbiol* 10:1408. <https://doi.org/10.3389/fmicb.2019.01408>.
55. Mariani M, Zimmerman C, Rodriguez P, Hasenohr E, Aimola G, Gerrard DL, Richman A, Dest A, Flamand L, Kaufer B, Fritze S. 2021. Higher-order chromatin structures of chromosomally integrated HHV-6A predict integration sites. *Front Cell Infect Microbiol* 11:612656. <https://doi.org/10.3389/fcimb.2021.612656>.
56. Xie K, Minkenberg B, Yang Y. 2015. Boosting CRISPR/Cas9 multiplex editing capability with the endogenous tRNA-processing system. *Proc Natl Acad Sci U S A* 112:3570–3575. <https://doi.org/10.1073/pnas.1420294112>.
57. Dong F, Xie K, Chen Y, Yang Y, Mao Y. 2017. Polycistronic tRNA and CRISPR guide-RNA enables highly efficient multiplexed genome engineering in human cells. *Biochem Biophys Res Commun* 482:889–895. <https://doi.org/10.1016/j.bbrc.2016.11.129>.
58. Hagag IT, Wight DJ, Bartsch D, Sid H, Jordan I, Bertzbach LD, Schusser B, Kaufer BB. 2020. Abrogation of Marek's disease virus replication using CRISPR/Cas9. *Sci Rep* 10:10919. <https://doi.org/10.1038/s41598-020-67951-1>.
59. van Diemen FR, Lebbink RJ. 2017. CRISPR/Cas9, a powerful tool to target human herpesviruses. *Cell Microbiol* 19:e12694. <https://doi.org/10.1111/cmi.12694>.
60. van Diemen FR, Kruse EM, Hooykaas MJG, Bruggeling CE, Schürch AC, van Ham PM, Imhof SM, Nijhuis M, Wiertz EJHJ, Lebbink RJ. 2016. CRISPR/Cas9-mediated genome editing of herpesviruses limits productive and latent infections. *PLoS Pathog* 12:e1005701. <https://doi.org/10.1371/journal.ppat.1005701>.
61. Roehm PC, Shekarabi M, Wollebo HS, Bellizzi A, He L, Salkind J, Khalili K. 2016. Inhibition of HSV-1 replication by gene editing strategy. *Sci Rep* 6:23146. <https://doi.org/10.1038/srep23146>.
62. Chen Y-C, Sheng J, Trang P, Liu F. 2018. Potential application of the CRISPR/Cas9 system against herpesvirus infections. *Viruses* 10:291. <https://doi.org/10.3390/v10060291>.
63. Aubert M, Strongin DE, Roychoudhury P, Loprieno MA, Haick AK, Klouser LM, Stensland L, Huang M-L, Makhosou N, Tait A, De Silva Feelixge HS, Galetto R, Duchateau P, Greninger AL, Stone D, Jerome KR. 2020. Gene editing and elimination of latent herpes simplex virus in vivo. *Nat Commun* 11:4148. <https://doi.org/10.1038/s41467-020-17936-5>.
64. Yuen KS, Chan CP, Wong NM, Ho CH, Ho TH, Lei T, Deng W, Tsao SW, Chen H, Kok KH, Jin DY. 2015. CRISPR/Cas9-mediated genome editing of Epstein-Barr virus in human cells. *J Gen Virol* 96:626–636. <https://doi.org/10.1099/jgv.0.000012>.
65. Peddu V, Dubuc I, Gravel A, Xie H, Huang ML, Tenenbaum D, Jerome KR, Tardif JC, Dubé MP, Flamand L, Greninger AL. 2019. Inherited chromosomally integrated human herpesvirus 6 demonstrates tissue-specific RNA expression *in vivo* that correlates with an increased antibody immune response. *J Virol* 94:e01418-19. <https://doi.org/10.1128/JVI.01418-19>.
66. Kumata R, Ito J, Sato K. 2020. Inherited chromosomally integrated HHV-6 possibly modulates human gene expression. *Virus Genes* 56:386–389. <https://doi.org/10.1007/s11262-020-01745-5>.
67. Kondo K, Shimada K, Sashihara J, Tanaka-Taya K, Yamanishi K. 2002. Identification of human herpesvirus 6 latency-associated transcripts. *J Virol* 76:4145–4151. <https://doi.org/10.1128/jvi.76.8.4145-4151.2002>.
68. Campbell A, Hogestyn JM, Folts CJ, Lopez B, Pröschel C, Mock D, Mayer-Pröschel M. 2017. Expression of the human herpesvirus 6A latency-associated transcript U94A disrupts human oligodendrocyte progenitor migration. *Sci Rep* 7:3978. <https://doi.org/10.1038/s41598-017-04432-y>.
69. Caruso A, Caselli E, Fiorentini S, Rotola A, Prandini A, Garrafa E, Saba E, Alessandri G, Cassai E, Di Luca D. 2009. U94 of human herpesvirus 6 inhibits *in vitro* angiogenesis and lymphangiogenesis. *Proc Natl Acad Sci U S A* 106:20446–20451. <https://doi.org/10.1073/pnas.0905535106>.
70. Caselli E, D'Accolti M, Caccuri F, Soffritti I, Gentili V, Bortolotti D, Rotola A, Cassai E, Fiorentini S, Zani A, Caruso A, Rizzo R, Di Luca D. 2020. The U94 gene of human herpesvirus 6: A narrative review of its role and potential functions. *Cells* 9:2608. <https://doi.org/10.3390/cells9122608>.
71. Rotola A, Ravaoli T, Gonelli A, Dewhurst S, Cassai E, Di Luca D. 1998. U94 of human herpesvirus 6 is expressed in latently infected peripheral blood mononuclear cells and blocks viral gene expression in transformed lymphocytes in culture. *Proc Natl Acad Sci U S A* 95:13911–13916. <https://doi.org/10.1073/pnas.95.23.13911>.
72. Readhead B, Haure-Mirande JV, Funk CC, Richards MA, Shannon P, Haroutunian V, Sano M, Liang WS, Beckmann ND, Price ND, Reiman EM, Schadt EE, Ehrlich ME, Gandy S, Dudley JT. 2018. Multiscale analysis of independent Alzheimer's cohorts finds disruption of molecular, genetic, and clinical networks by human herpesvirus. *Neuron* 99:64–82.e7. <https://doi.org/10.1016/j.neuron.2018.05.023>.
73. Westman G, Blomberg J, Yun Z, Lannfelt L, Ingelsson M, Eriksson BM. 2017. Decreased HHV-6 IgG in Alzheimer's disease. *Front Neurol* 8:40. <https://doi.org/10.3389/fneur.2017.00040>.
74. Carbone I, Lazzarotto T, Ianni M, Porcellini E, Forti P, Masliah E, Gabrielli L, Licastro F. 2014. Herpes virus in Alzheimer's disease: relation to progression of the disease. *Neurobiol Aging* 35:122–129. <https://doi.org/10.1016/j.neurobiolaging.2013.06.024>.
75. Ortega-Madueño I, Garcia-Montojo M, Dominguez-Mozo MI, Garcia-Martinez A, Arias-Leal AM, Casanova I, Arroyo R, Alvarez-Lafuente R. 2014. Anti-human herpesvirus 6A/B IgG correlates with relapses and progression in multiple sclerosis. *PLoS One* 9:e104836. <https://doi.org/10.1371/journal.pone.0104836>.
76. Alenda R, Álvarez-Lafuente R, Costa-Frossard L, Arroyo R, Mirete S, Álvarez-Cermeño JC, Villar LM. 2014. Identification of the major HHV-6 antigen recognized by cerebrospinal fluid IgG in multiple sclerosis. *Eur J Neurol* 21:1096–1101. <https://doi.org/10.1111/ene.12435>.
77. Lundström W, Gustafsson R. 2022. Human herpesvirus 6A is a risk factor for multiple sclerosis. *Front Immunol* 13:840753. <https://doi.org/10.3389/fimmu.2022.840753>.
78. Romanescu C, Schreiner TG, Mukovozov I. 2022. The role of human herpesvirus 6 infection in Alzheimer's disease pathogenicity—a theoretical mosaic. *J Clin Med* 11:3061. <https://doi.org/10.3390/jcm11113061>.
79. Wood ML, Royle NJ. 2017. Chromosomally integrated human herpesvirus 6: models of viral genome release from the telomere and impacts on human health. *Viruses* 9:184. <https://doi.org/10.3390/v9070184>.
80. Collin V, Flamand L. 2017. HHV-6A/B integration and the pathogenesis associated with the reactivation of chromosomally integrated HHV-6A/B. *Viruses* 9:160. <https://doi.org/10.3390/v9070160>.
81. Prusty BK, Krohne G, Rudel T. 2013. Reactivation of chromosomally integrated human herpesvirus-6 by telomeric circle formation. *PLoS Genet* 9:e1004033. <https://doi.org/10.1371/journal.pgen.1004033>.
82. Borenstein R, Zeigerman H, Frenkel N. 2010. The DR1 and DR6 first exons of human herpesvirus 6A are not required for virus replication in culture and are deleted in virus stocks that replicate well in T-cell lines. *J Virol* 84:2648–2656. <https://doi.org/10.1128/JVI.01951-09>.
83. Everett RD, Rechter S, Papior P, Tavalai N, Stamminger T, Orr A. 2006. PML contributes to a cellular mechanism of repression of herpes simplex virus type 1 infection that is inactivated by ICPO. *J Virol* 80:7995–8005. <https://doi.org/10.1128/JVI.00734-06>.
84. Sanyal A, Wallaschek N, Glass M, Flamand L, Wight DJ, Kaufer BB. 2018. The ND10 complex represses lytic human herpesvirus 6A replication and promotes silencing of the viral genome. *Viruses* 10:401. <https://doi.org/10.3390/v10080401>.
85. van de Weijer ML, Bassik MC, Luteijn RD, Voorburg CM, Lohuis MAM, Kremmer E, Hoebe RC, LeProust EM, Chen S, Hoelen H, Rensing ME, Patena W, Weissman JS, McManus MT, Wiertz EJHJ, Lebbink RJ. 2014. A

- high-coverage shRNA screen identifies TMEM129 as an E3 ligase involved in ER-associated protein degradation. *Nat Commun* 5:3832. <https://doi.org/10.1038/ncomms4832>.
86. Phizicky EM, Hopper AK. 2010. tRNA biology charges to the front. *Genes Dev* 24:1832–1860. <https://doi.org/10.1101/gad.1956510>.
87. Schiffer S, Rösch S, Marchfelder A. 2002. Assigning a function to a conserved group of proteins: the tRNA 3'-processing enzymes. *EMBO J* 21:2769–2777. <https://doi.org/10.1093/emboj/21.11.2769>.
88. Barbezier N, Canino G, Rodor J, Jobet E, Saez-Vasquez J, Marchfelder A, Echeverría M. 2009. Processing of a dicistronic tRNA-snoRNA precursor: combined analysis in vitro and in vivo reveals alternate pathways and coupling to assembly of snoRNP. *Plant Physiol* 150:1598–1610. <https://doi.org/10.1104/pp.109.137968>.
89. Kruszka K, Barneche F, Guyot R, Ailhas J, Meneau I, Schiffer S, Marchfelder A, Echeverría M. 2003. Plant dicistronic tRNA-snoRNA genes: a new mode of expression of the small nucleolar RNAs processed by RNase Z. *EMBO J* 22:621–632. <https://doi.org/10.1093/emboj/cdg040>.
90. Heckl D, Kowalczyk MS, Yudovich D, Belizaire R, Puram RV, McConkey ME, Thielke A, Aster JC, Regev A, Ebert BL. 2014. Generation of mouse models of myeloid malignancy with combinatorial genetic lesions using CRISPR-Cas9 genome editing. *Nat Biotechnol* 32:941–946. <https://doi.org/10.1038/nbt.2951>.
91. Ran FA, Hsu PD, Wright J, Agarwala V, Scott DA, Zhang F. 2013. Genome engineering using the CRISPR-Cas9 system. *Nat Protoc* 8:2281–2308. <https://doi.org/10.1038/nprot.2013.143>.
92. Kaufer BB. 2013. Detection of integrated herpesvirus genomes by fluorescence in situ hybridization (FISH), p 141–152. *In* Bailer SM, Lieber D (ed), *Virus-host interactions: methods and protocols*. Humana Press, Totowa, NJ.
93. Aswad A, Aimola G, Wight D, Roychoudhury P, Zimmermann C, Hill J, Lassner D, Xie H, Huang ML, Parrish NF, Schultheiss HP, Venturini C, Lager S, Smith GCS, Charnock-Jones DS, Breuer J, Greninger AL, Kaufer BB. 2021. Evolutionary history of endogenous human herpesvirus 6 reflects human migration out of Africa. *Mol Biol Evol* 38:96–107. <https://doi.org/10.1093/molbev/msaa190>.